Legends of the Supplemental Data:

Supplemental Figure 1. p-NK-cells are phenotypically altered in breast cancer patients.

Mono-parametric histogram representative of p-NK-cell phenotype in patients displaying different stages of breast cancer. B = mammary benign tumors; Tis = non-invasive in situ breast cancer; LOC = localized invasive breast cancer; LA = locally-advanced invasive breast cancer; M = metastatic breast cancer.

Supplemental Figure 2. **p-NK-cells are functionally altered in breast cancer patients.**

A. Titration curves of NK-cells ability to mediate ADCC in the presence of increasing doses of trastuzumab. The effect of trastuzumab was measured through the degranulation (CD107) ability of p-NK-cells. Effector:Target ratio = 2:1, in a 4 hours assay. n=3 donors. **B**. *CD16* polymorphism was evaluated in the population by flow cytometry (*CD16* polymorphism affinity: VV>VF>FF, Personal communication from Dr Thibault, manuscript in preparation). For all experiments, the Effector:Target ratio was of 1:1. The number of patients included per group was as follows: B (n=10), Tis (n=7), LOC (n=16), LA (n=16), M (n=12). **C-D**.NK-cells were stimulated in a re-directed assay, using P815 cell lines pre-coated with anti-NKp30 or anti-CD16 agonist antibody, and their functions evaluated by their ability to express membrane CD107 molecules (de-granulation assay) when exposed to target cells. The correlation between the expression level of NKp30 (**C**) or CD16 (**D**) and the respective CD107 degranulation ability were established using the non-parametric Spearman correlation test. For all experiments, the Effector:Target ratio was of 1:1.

The statistical differences between groups were established using non-parametric Mann and Whitney t-test. p-values<0.05 were considered as significant. ns=not significant. p<0.05=*; p≤0.05=**; p≤0.0005=***.

Supplemental Figure 3. Phenotype of healthy or malignant mammary tissues infiltrating NK-cells and peripheral-blood NK-cells.

A. Expression of NK-cells receptors on healthy Mt-NK, linked to their paired Ti-NK, and p-NK. Markers significantly altered in the healthy mammary tissue compared to p-NK (tissue-induced modifications) are squared in green. The statistical differences between groups were established using paired non-parametric Wilcoxon t-test. **B**. Correlation curves between the MFI of NKp30, CD16, NKG2A and CD16 on p-NK-cells and Ti-NK-cells (n = 11). Statistical analysis and correlation coefficients were established with non-parametric Spearman tests. p-values<0.05 were considered as significant. ns=not significant. p<0.05=*; p≤0.05=**; p≤0.0005=***.

Supplemental Figure 4. mRNA expression of the known NK-cell receptor ligands in breast cancer. Affymetrix data of breast cancers (n= 250) and healthy mammary tissue (n=5) were downloaded from the public GEO datasets (GEO:http://www.ncbi.nlm.nih.gov.gate2.inist.fr/pubmed/, GSE21653). We used the Robust Multichip Average (RMA) with the non-parametric quantile algorithm as normalization parameter. Quantile normalization or RMA was done in R using Bioconductor and associated packages. mRNA values of the NK-cell receptor ligands were extracted, centered on healthy mammary tissue to obtain the differential expression and then submitted to a clustering software (Cluster®: linearization of the data, mean centered on gene); the results are visualized with Treeview®. The

receptors of the known ligands of interest are: KIRs (HLA-A, HLA-B, HLA-C, HLA-G), NKG2A (HLA-E), NKp30 (BAT-3, B7H6 or NKp30L), DNAM-1 (PVR and Nectin2), NKG2D (MIC-A, MIC-B, ULBP-1, ULBP-2 and ULBP-3). Healthy mammary tissue cluster are squared in yellow dashed line.

Supplemental Figure 5. Levels of TGF-β1, PGE_2, LGALS3 , ADAM17 and sMICA in malignant and healthy breast tissues measured by ELISA.

A. TGF-β1; **B.** PGE_2; **C.** LGALS3; **D.** ADAM17; **E.** sMICA;

Supplemental Figure 6. The proportion of Treg infiltrates were negatively correlated with the cytotoxic molecules CD57 and GZMB expressed in Ti-NK-cells.

A. Percentage of Treg in p-blood, healthy mammary tissue and in tumor. **B**. Correlation between Treg infiltrates and CD57 expression on NK-cells. **C.** Correlation between Treg infiltrates and GZMB expression on NK-cells. Statistics and correlation coefficient were established with non-parametric Pearson tests. p-values<0.05 were considered as significant. ns=not significant. p<0.05=*; p≤0.05=**; p≤0.0005=***.

Supplemental Figure 7. **Tumor cells alter NK-cells phenotype and function in the MMTV-Neu murine model of breast cancer.**

FVB control mice (n=6, light grey bars) and MMTV-Neu mice (n=6, dark grey bars) were followed from 3 months of age until tumor occurrence, and a Kaplan-Meier curve was established to determine tumor-free survival (**A**). Arrows indicate when the samples were collected. Mice were sacrificed during the last sample (VI). NKp46 (**B**) and NKG2A (**C**) expression were followed on NK-cells from FVB and MMTV-Neu

mice. FVB and MMTV/Neu mice were compared using non-parametric Mann and Whitney t-test. p-values<0.05 were considered as significant. $p<0.05$=*; $p\leq0.005$=**; $p\leq0.0005$=***.

Supplemental Table 1. List of the antibodies (Name, Clone, Provider) used for NK-cells phenotype and functional experiments.

mAb	Clone	Provider
anti-CD3	UCHT1	Beckman Coulter
anti-CD4	13B8.2	Beckman Coulter
anti-CD16	3G8	Beckman Coulter
anti-CD56	N901	Beckman Coulter
anti-NKp30	7A6	Beckman Coulter
anti-NKG2D	BAT-221	Beckman Coulter
anti-NKp46	BAB281	Beckman Coulter
anti-NKp44	Z231	Beckman Coulter
anti-2B4	PP35	Beckman Coulter
anti-NKG2A	Z270	Beckman Coulter
anti-NKG2D	ON72	Beckman Coulter
anti-CD158a	11PB6	Beckman Coulter
anti-CD158b	GL183	Beckman Coulter
anti-CD158e	Z27	Beckman Coulter
anti-CD158i	FES172	Beckman Coulter
anti-NTBA	MA127	Beckman Coulter
anti-LFA1	JT90	Beckman Coulter
anti-CD85j	HP-F1	Beckman Coulter
anti-CD2	39C1.5	Beckman Coulter
anti-CD161	191B8	Beckman Coulter
anti-CD57	NC1	Beckman Coulter
anti-CD25	B1.49.9	Beckman Coulter
anti-CD27	1A4CD27	Beckman Coulter
anti-CD69	TP1.55.3	Beckman Coulter
anti-CD127	R34.34	Beckman Coulter
anti-HLA-ABC	B9.12.1	Beckman Coulter
anti-IFN-gamma	45.15	Beckman Coulter
anti-DNAM-1	F22	BD Pharmingen
anti-Perforin	δG9	BD Pharmingen
anti-Granzyme-B	GB11	BD Pharmingen
anti-CD31	M89D3	BD Pharmingen
anti-TNF-alpha	6401.1111	BD Pharmingen
anti-MIC-A/B	6D4	BD Pharmingen
7-AAD		BD Pharmingen
anti-TRAIL	75402	R&D System
anti-NKG2C	134591	R&D System
anti-NKp80	239127	R&D System
anti-LAIR	342219	R&D System
DNAM-1-FC	recombinant	R&D System
NKp30-Fc	recombinant	R&D System
anti-ULBP1	170818	R&D System
anti-ULBP2	165903	R&D System
anti-ULBP3	166510	R&D System
anti-HLA-E	3D12HLA-E	eBioscience

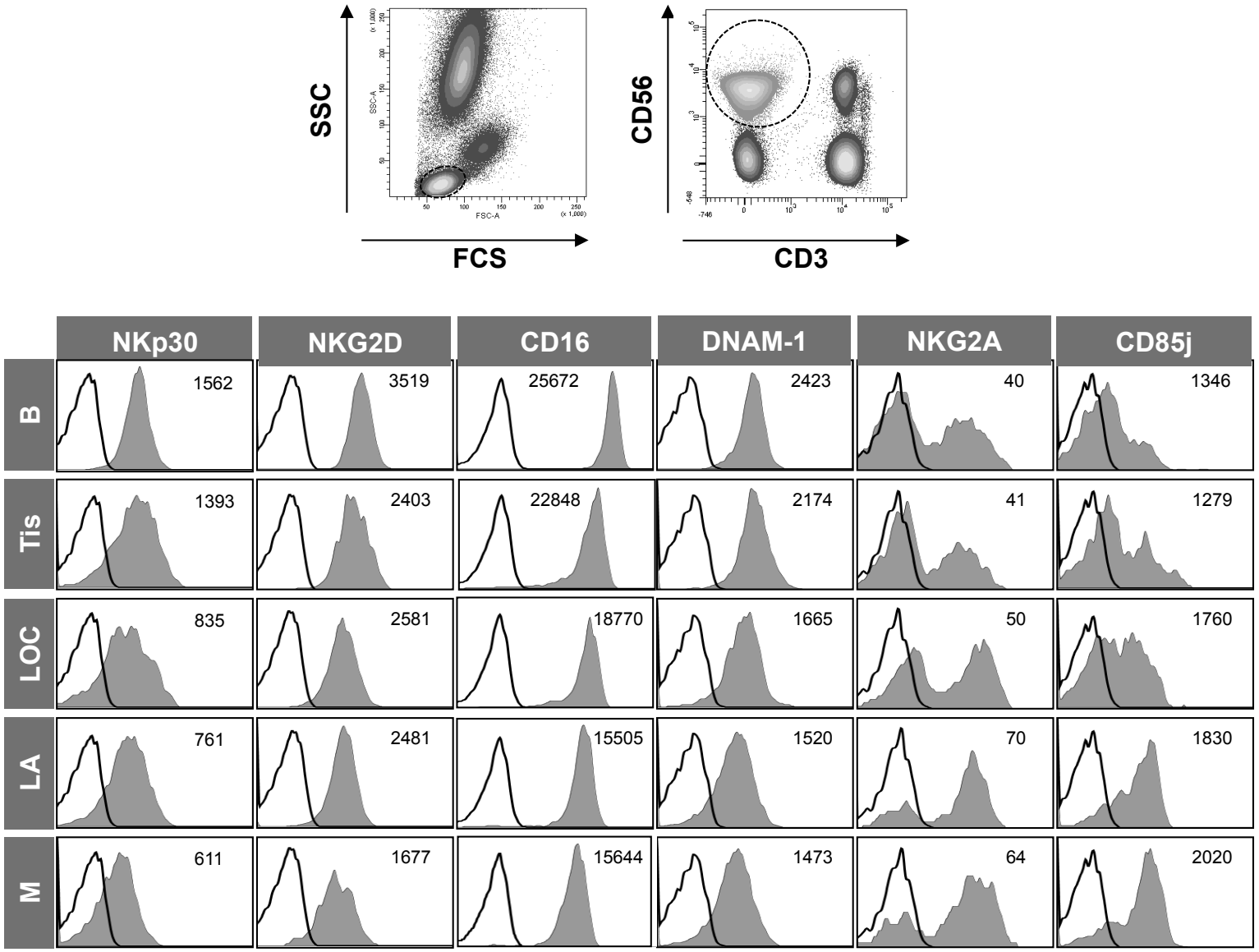

Supplemental Figure 1. p-NK-cells are phenotypically altered in breast cancer patients.

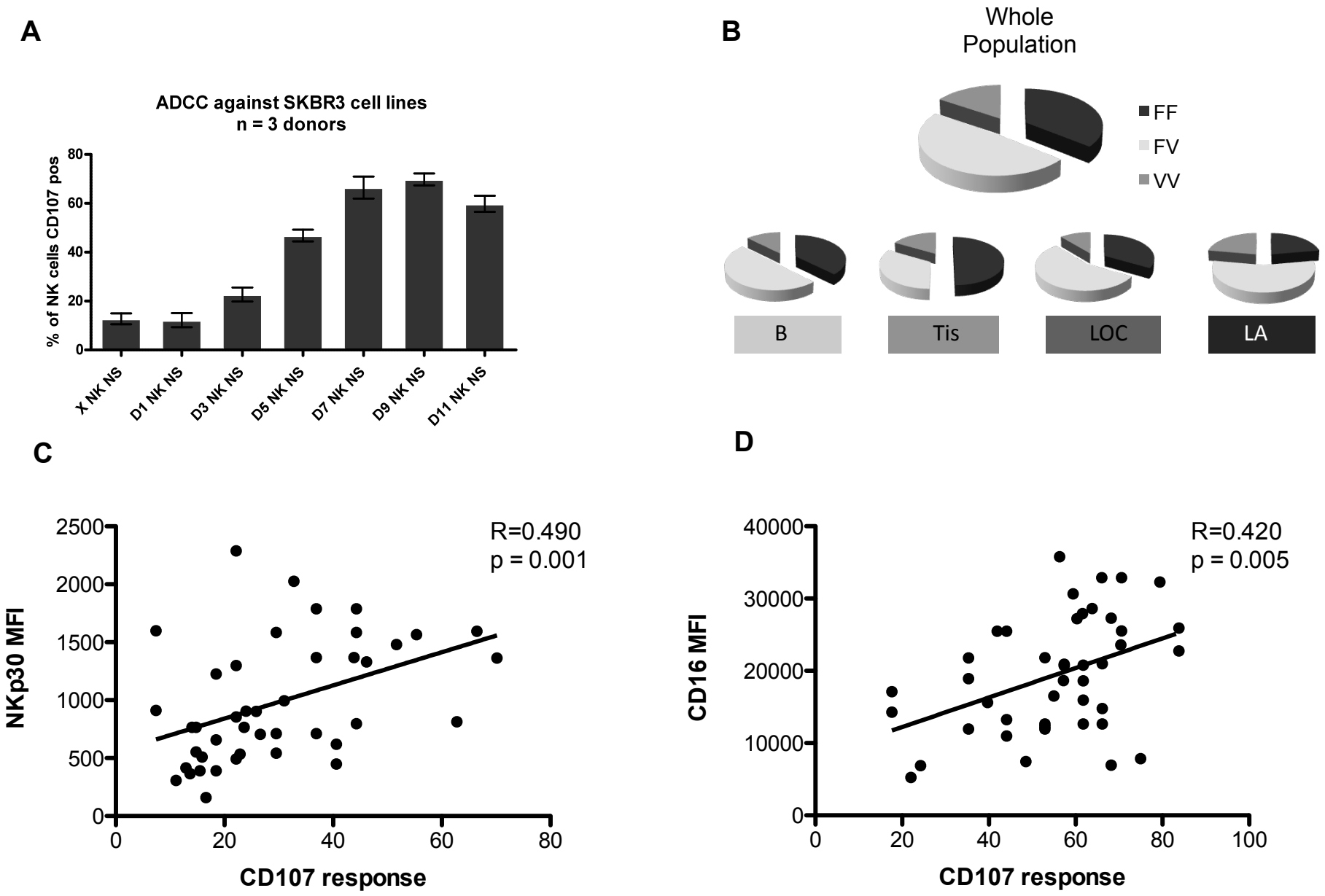

Supplemental Figure 2. p-NK-cells are functionally altered in breast cancer patients.

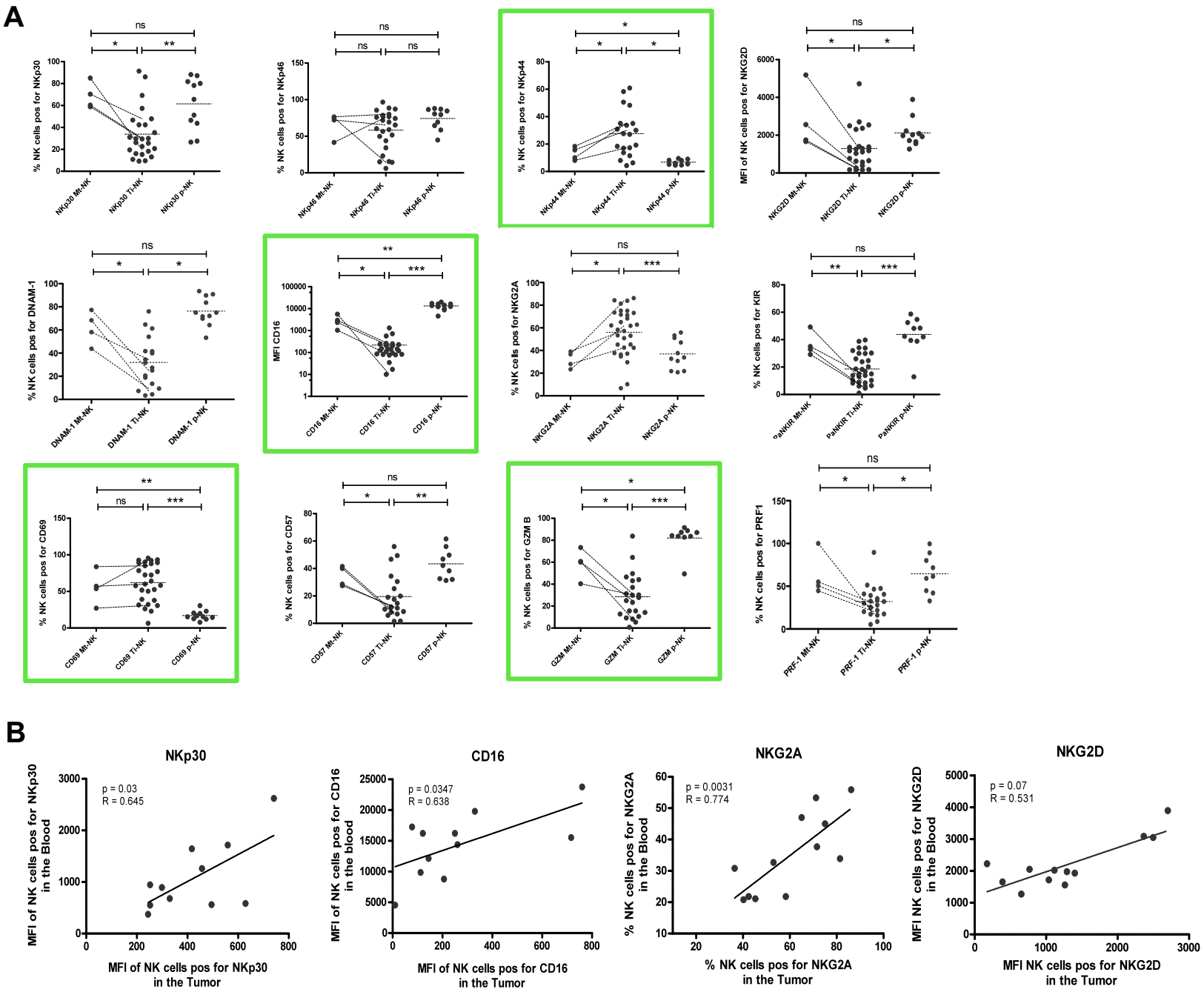

Supplemental Figure 3. Phenotype of tissues infiltrating and peripheral blood NK-cells.

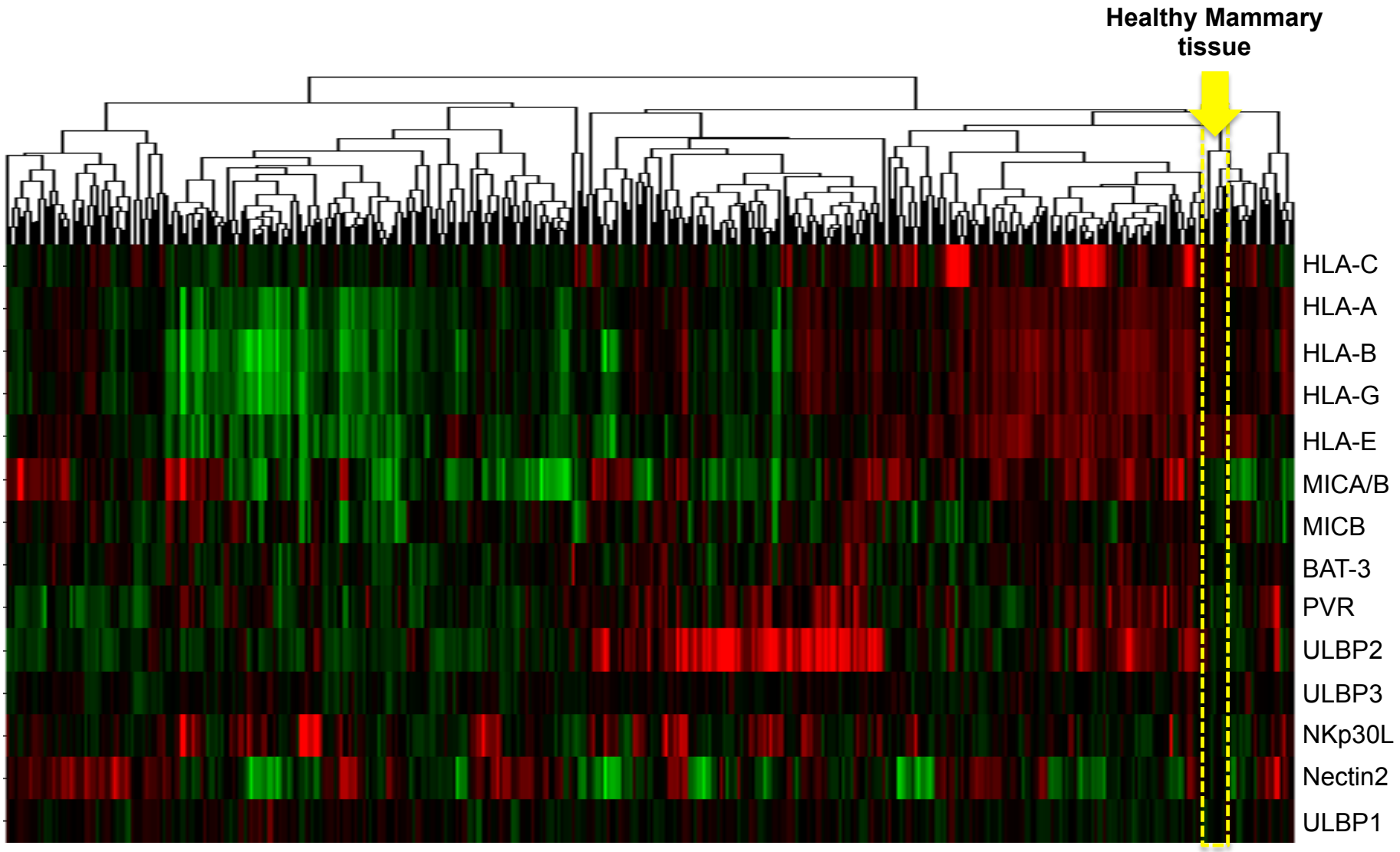

Supplemental Figure 4. mRNA expression of the known NK-cell receptor ligands in breast cancer.

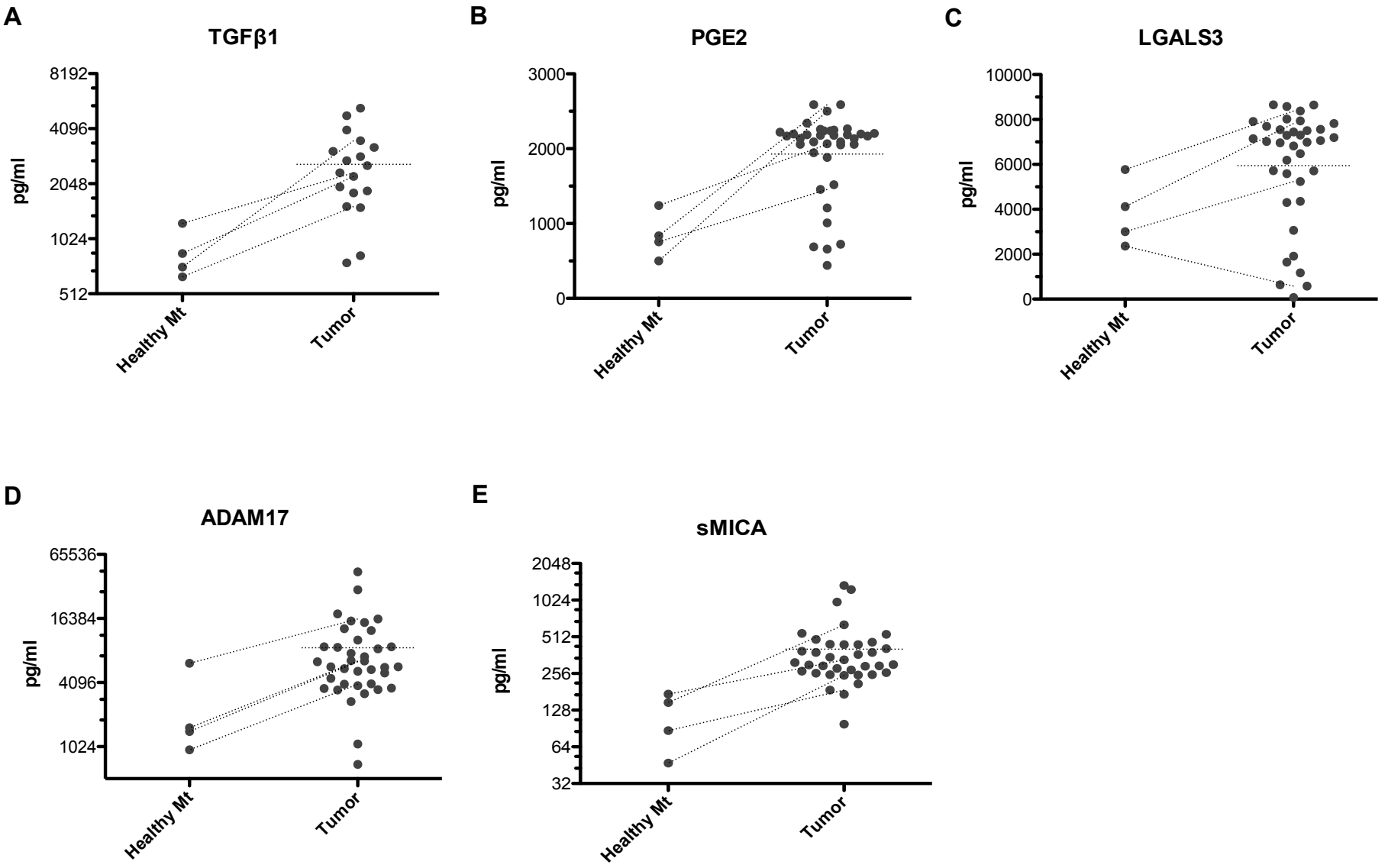

Supplemental Figure 5. Levels of TGF-b1, PGE_2, LGALS3, ADAM17 and sMICA in malignant and healthy breast tissues measured by ELISA.

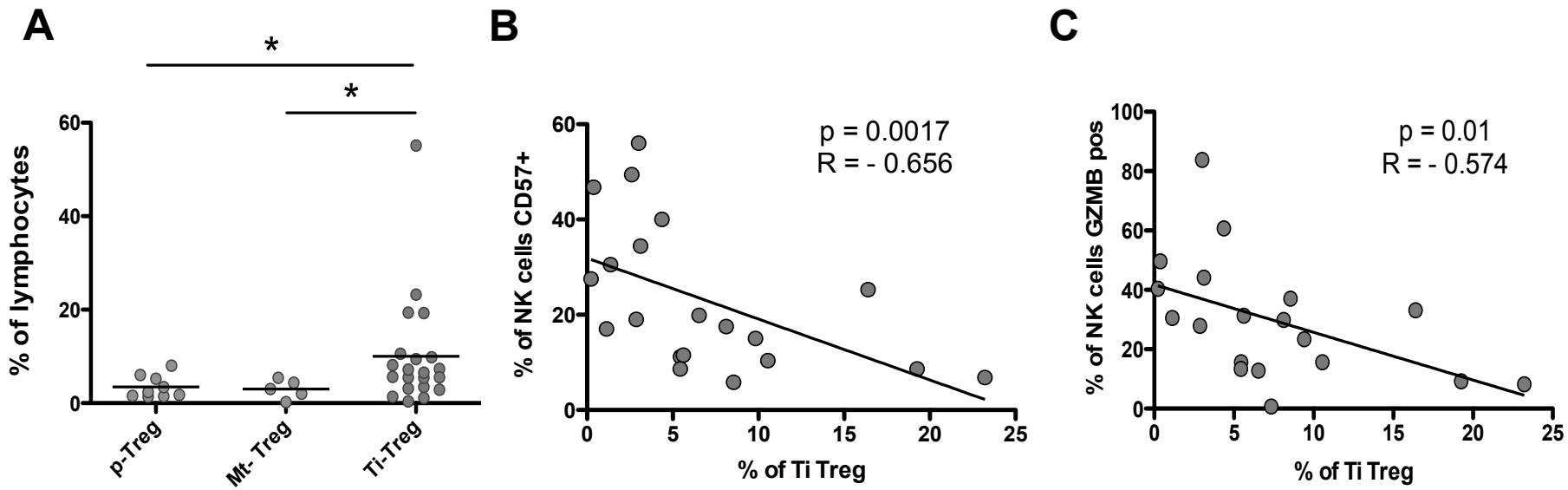

Supplemental Figure 6. The proportion of Treg infiltrates were negatively correlated with the cytotoxic molecules CD57 and GZMB expressed in Ti-NK-cells.

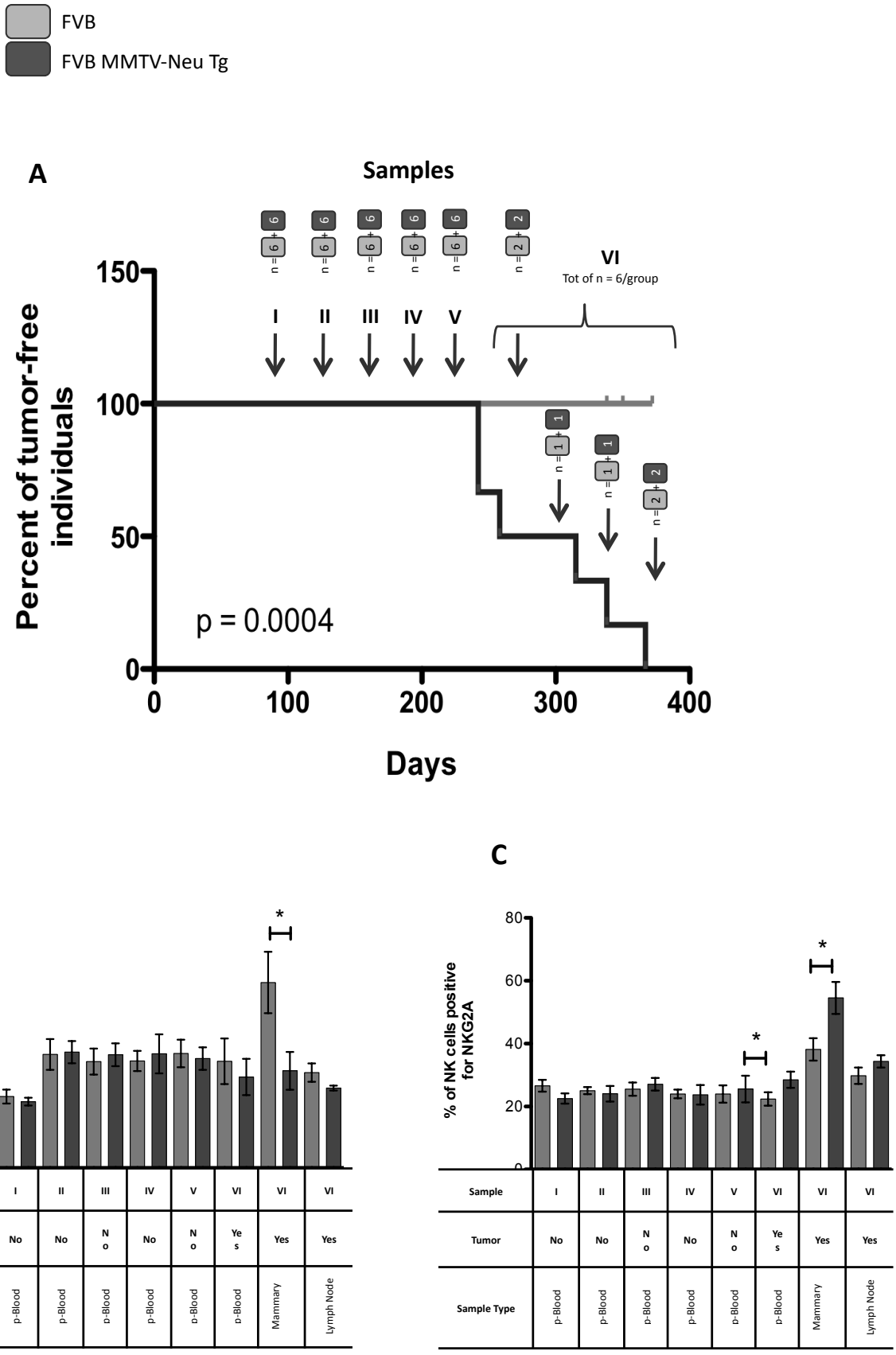

Supplemental Figure 7. Tumor cells alter NK-cells phenotype and function in the MMTV-Neu murine model of breast cancer.